Iranian Journal of Materials Forming 9 (3) (2022) 4-17

Online ISSN: 2383-0042

IJMF

Iranian Journal of Materials Forming

Journal Homepage: http://ijmf.shirazu.ac.ir

Research Article

The Effects of the Thermo-Mechanical Process Variables on the Microstructure, Mechanical Properties, and Recrystallization Behavior of the Commercially Pure Titanium

Y. Mazaheri[1*], K. Ahmadi[2], M.M. Jalilvand[2], M. Bahiraei[2] and M. Sheikhi[2]

[1] Department of Materials Science and Engineering, School of Engineering, Shiraz University, Shiraz, 71946-84334, Iran
[2] Department of Materials Engineering, Bu-Ali Sina University, Hamedan, 65178-38695, Iran

ARTICLE INFO

Article history:

Received 16 March 2022
Reviewed 5 April 2022
Revised 11 April 2022
Accepted 11 April 2022

Keywords:

Commercially pure titanium
Cold-rolling
Annealing
Recrystallization
Mechanical properties

ABSTRACT

Commercial pure titanium sheets were thermo-mechanically treated to investigate the effects of the treatment variables on the microstructure, mechanical properties, and recrystallization behavior. The as-received sheets were initially cold-rolled up to different reduction percentages of 60%, 75%, and 90%. Then, the cold-rolled samples were annealed at different temperatures of 500°C-700°C, for various time ranges of 5 to 60 minutes. The evolution of the microstructure of the samples was studied using X-ray diffraction analysis and optical microscopy. The hardness of the 90% cold-rolled sample was about 82% higher than that of the as-received sheet. Increasing the time and temperature of the annealing process caused a decrease in the microhardness values of the samples. The recrystallization activation energy and Avrami's exponent of the 90% cold-rolled sample were calculated as about 179 kJ/mol and 0.75, respectively. The results of the uniaxial tensile tests revealed that the cold-rolling process significantly improved the yield strength (YS) and ultimate tensile strength (UTS) of the specimens. In the case of the 90% cold-rolled sample, these values improved by about 160% and 117% with respect to the as-received metal, respectively. However, the elongation of the cold-rolled samples dropped sharply. Moreover, annealing had a positive effect on the elongation of the cold-rolled samples. The UTS and elongation percentage of the as-received sheet were 415 MPa and 36.4%, respectively. These values were varied to 558 MPa and 29.15% for the 90% cold-rolled sample annealed at 700°C for 1 h. To study the fracture behavior of the different samples, scanning electron microscopy (SEM) was used.

1. Introduction

Due to the fact that titanium has a desirable mixture of characteristics such as high strength-weight ratio, high fracture toughness, excellent corrosion resistance, and proper biocompatibility, it is becoming a material of choice in chemical, aerospace, and biomaterials applications [1, 2]. Commercially pure titanium (CP Ti) has a hexagonal close-packed (HCP) lattice structure at room temperature, which is characterized by few independent easy deformation systems and a low lattice structure symmetry [3]. These properties play an

* Corresponding author
E-mail address: yousef.mazaheri@shirazu.ac.ir (Y. Mazaheri)
https://doi.org/10.22099/IJMF.2022.43343.1220

important role in the mechanical and physical characteristics of titanium.

Developing fine grain metals is the most effective approach to simultaneously improve strength and ductility. This approach can be carried out through severe plastic deformation (SPD) methods and thermo-mechanical processes (TMPs). TMPs alter the microstructure of the materials and induce a new crystallographic texture in them. Since TMPs consist of a plastic deformation stage, it activates the most favorably twinning or oriented slip systems [4]. The plastic deformation changes grain shape, induce hardening phenomena, increase the dislocation density, and alter the corrosion performance as well as the thermal and electrical conductivities [5].

When the deformed material is subsequently annealed, the recrystallization phenomenon begins by nucleation at preferred sites of the deformed microstructure. Then, these newly nucleated grains start to grow with a texture influenced by the local orientations in the microstructure. The final recrystallized grains are known as recrystallization textures [4]. Although a major portion of the energy transferred to the material during the process of deformation spoils as heat, a considerable portion of energy remains stored in the material. During the grain growth step, the energy stored during the deformation stage can be partially or completely removed [5].

Since the final texture is derived from the deformation texture, the conditions of the deformation process have a significant effect on the recrystallized texture. Specifically, the change in rolling reduction percentages leads to the fabrication of materials with a distinct defect structure which consists of different textures, microstructure, and residual stress. Additionally, it should be mentioned that the deformation conditions will affect the mechanical properties of the CP Ti derived from TMPs, as studied by a few researchers [6, 7].

The TMPs conditions significantly affect the deformation texture and subsequently the final recrystallized texture of the crystalline materials. The deformation type, deformation mode, strain rate, strain path, annealing temperature, annealing time, and also cooling behavior are important parameters of the TMPs. These parameters also induce the different levels of residual stresses in the metal [8, 9]. Most studies in the field of the TMPs have been concerned with metals that have cubic symmetry, such as ferrous alloys and aluminum-based alloys. Recrystallization behavior and texture in structural HCP materials, including magnesium, zirconium, and titanium, must be explored. In these metals, in addition to basal or prismatic slip systems, twinning is also activated to accommodate the plastic strain along the c-axis [10, 11].

Various studies have been done on the mechanical properties and microstructure of the deformed titanium by different processes. However, research about the behaviors of the recrystallization kinetics of these alloys is still needed to be deeply investigated. The importance of investigating the kinetics behavior of the recrystallization is the close connections between the type of deformation, time, and temperature of the annealing process which directly affects the recrystallization behavior and consequently microstructure and mechanical performances of the alloy. Thus, the present study aims to investigate the effect of thermo-mechanical processing parameters such as thickness reduction percentage of the rolling process, annealing temperature, and annealing time on the microstructure of the CP Ti sheets. In addition, the influence of the mentioned parameters on the mechanical performance and recrystallization behavior of the samples was evaluated.

2. Experimental Procedure

2.1. Materials

The as-received CP Ti sheets with dimensions of 50 mm (length) × 30 mm (width) × 7 mm (thickness) were used to conduct experiments. The chemical composition of the sheet is given in Table 1.

Table 1. Chemical composition of the CP Ti sheets (wt.%)

Fe	S	O	N	C	Ti
0.03	0.01	0.18	0.01	0.10	Bal.

2.2. Methods

To investigate the effects of TMP variables on the CP Ti sheets, they were initially cold-rolled up to 60%, 75%, and 90% reduction in thickness. The cold-rolling process was carried out on the samples using a two-roll rolling machine (2RM-125D). The process was done in a constant rolling direction. Additionally, industrial lubricant was performed on the samples after each pass of rolling. After the cold-rolling process, the rolled sheets were annealed at 500°C-700°C for 5, 15, 25, and 60 min in an electrical resistance furnace. The ranges of annealing temperatures and times were chosen according to the previous studies [3, 12]. Fig. 1 schematically shows the experimental procedure which was carried out in this study.

2.3. Characterization

First, to investigate the microstructure of the samples including as-received, cold-rolled, and annealed, they were sand gritted, polished, and then etched for 25 s by Kroll's reagent (10 vol.% HF, 10 vol.% HNO_3, and 80 vol.% distilled water). The microstructural investigations were carried out on the samples using Union Versa met-2 optical microscope. The grain size of the as-received CP Ti, and 90% cold-rolled samples, was determined using metallographic image processing (MIP) software.

To calculate the crystallite size and dislocation density of the cold-rolled samples, X-ray diffraction (XRD) analysis with a Cu Kα radiation (λ= 0.1506 nm) was performed utilizing a Rigaku (Germany) instrument. The step size, 2θ range, and counting time of the XRD tests were 0.02°, 10°-110°, and one second per step, respectively. The crystallite size and dislocation density were calculated by the XRD line profile analysis (XRD-LPA) using MAUD software based on the Rietveld method [13].

To measure the hardness of the samples, the Vickers's micro hardness test was performed on them using (SM310-E, Japan). The applied force and indentation time was 3 N, and 25 s, respectively. The average of at least five measurements was reported as the microhardness value for each sample.

To study the mechanical performances of the samples, tensile tests were carried out along their rolling direction. The tensile specimens were prepared using the electro-discharge machining (EDM) technique according to the ASTM A370 standard. The gauge length, gauge width, and thickness of the tensile specimens were 20 mm, 5 mm, and 1.2 mm, respectively. The uniaxial tensile tests were done by the SANTAM STM60 machine at a constant movement speed of 1 mm/min. Each test was repeated three times, and the average of three measurements was reported in the text in order to ensure the repeatability of the process. Moreover, the fracture surface of the samples was analyzed by scanning electron microscopy (SEM, JEOL JSM-840) to secure a more proper understanding of the fracture mechanism and tensile behavior of the samples.

3. Results and Discussion

3.1. Microstructural evolutions

The microstructure of the as-received CP Ti is illustrated in Fig. 2. The microstructure consists of α-equiaxed grains. The average size of α-grains was 35±5 µm. The twinning is marked by yellow arrows in Fig. 2.

Fig. 3 presents XRD patterns obtained for the as-received and cold-rolled samples. As illustrated in Fig. 3, the patterns indicate typical diffraction peaks attributed

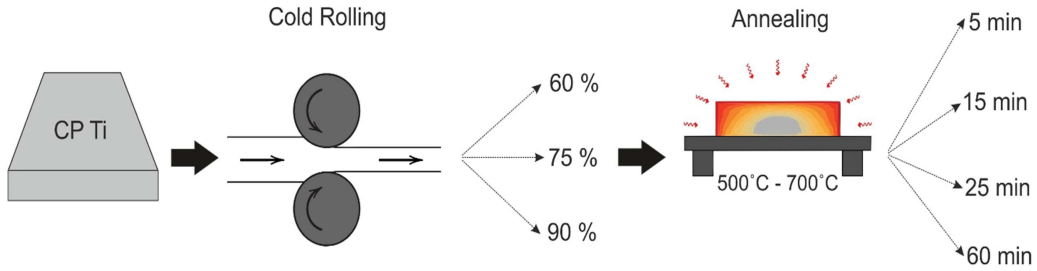

Fig. 1. The schematics illustrating the experimental procedure carried out in the present study.

to the CP Ti which has HCP crystal microstructure. In the XRD patterns of the cold-rolled samples, peak broadening can be observed. Furthermore, the intensities of the related peaks in the case of the cold-rolled samples were reduced. These two facts are an indication of the reduction of the crystallite size. Inversely, the peak broadening can be considered as a sign of an increase in the lattice strain induced to the metal during deformations. Increasing the reduction percentage, causes the peak broadening phenomena to become more apparent.

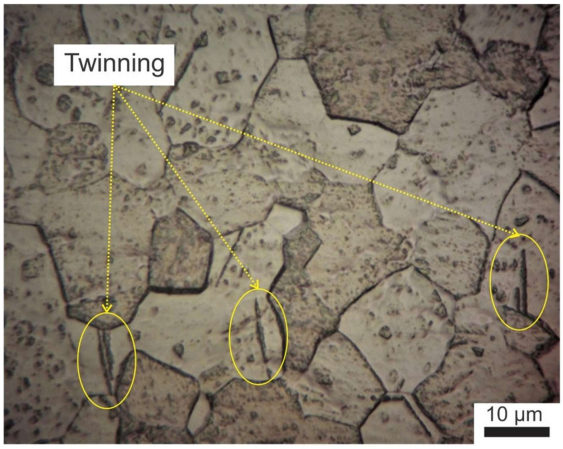

Fig. 2. Microstructure of as-received CP Ti (grade 2).

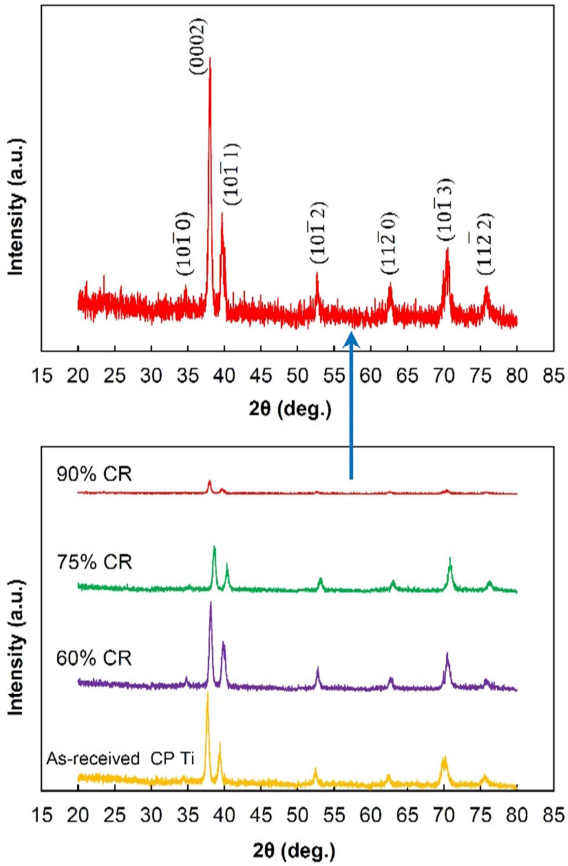

Fig. 3. XRD patterns of the as-received and cold-rolled CP Ti samples at different percentage of reduction.

It was proposed that during the cold-rolling process, firstly, the primary grains are subdivided to form sub-grains or low angle grain boundaries (LAGBs). Continuing the process increases the misorientation and dislocation accumulation. This changes the LAGBs to high-angle grain boundaries (HAGBs). Eventually, the HAGBs migrate and establish the well-defined UFG structures [14]. Thus, the cold-rolling process can cause the formation of the ultra-fine and nanograins structures in the pure titanium [15].

Fig. 4 presents values of the crystallite size, and dislocation density of the cold-rolled CP Ti samples calculated using XRD data. The values of crystallite size (D) and lattice microstrain (ε) were obtained using MAUD software based on the Rietveld method [13]. Moreover, the dislocation density (ρ) was measured using Eq. (1) in which b is Berger's vector [16]:

$$\rho = \frac{3\sqrt{2\pi}(\varepsilon^2)^{1/2}}{Db} \quad (1)$$

As expected, the crystallite size showed a decreasing trend once the reduction percentage of the cold-rolling process was increased. On the other hand, the dislocation density became greater by performing more passes of the

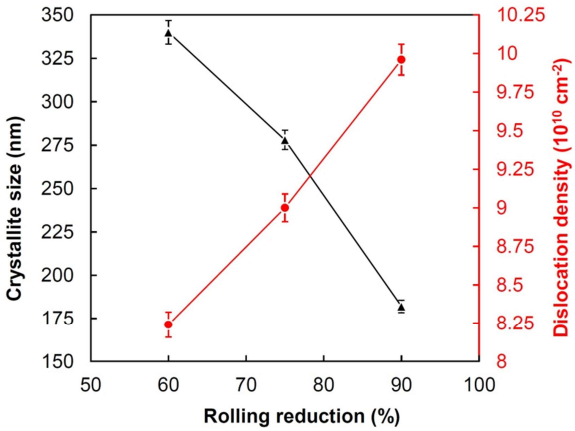

Fig. 4. The variations of the crystallite size and dislocation density by the reduction percentage of the cold-rolling process obtained from XRD analysis.

cold-rolling process. The cold-rolling process induces lattice strain in the samples which, regarding Eq. (1), causes the dislocation density to increase.

Fig. 5 displays the microstructures of the 90% cold-rolled sample after being annealed at 500°C, and 700°C for different annealing times (900, 1500, and 3600 s). It is obvious that the amount of dynamic recrystallization increased by lasting the annealing time. Annealing at 700°C causes the evolution of spherical α-grains. After annealing, the number of twins significantly decreased, and the recrystallized grains grew. Annealing at longer times and higher temperatures caused a larger growth in recrystallized grains. After one hour of annealing, an equiaxed grain structure was generated and the deformed structure faded away (Figs. 5(c) and 5(f)), meaning the recrystallization was completed at this annealing condition. The evolution of a new array of the non-deformed equiaxial grains originated from the small nuclei is called recrystallization. The small nuclei continue to grow until the original deformed matrix is entirely replaced with the new grains which have low dislocation density [12]. The energy stored in such dislocations is considered as the driving force for the primary recrystallization.

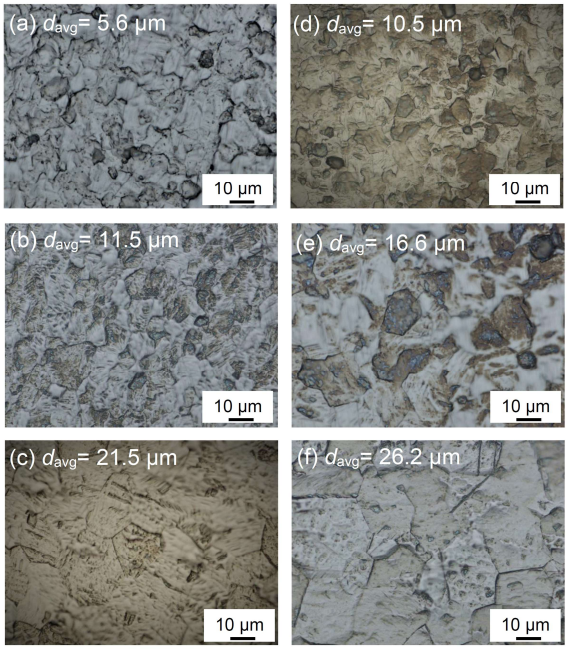

Fig. 5. Microstructure of the 90% cold-rolled sample after annealing at 500°C (a-c) and 700°C (d-f) for 900 s (a, d), 1500 s (b, e), and 3600 s (c, f).

Regions with higher free energy density, are the most likely sites for the emergence of recrystallized grains. The amount of strain energy stored in materials in the form of imperfections, such as line defects (dislocations) and point defects (vacancies), determines the number of suitable sites for activation of the nucleation process in the matrix. When a metal is extremely cold worked, the number of these sites increases [17]. It was reported that performing the cold-rolling process at a high reduction percent results in the formation of an equiaxed grain with a fine distribution after annealing the titanium [3]. Therefore, the cold working conditions determine the annealing and recrystallization behavior in polycrystalline titanium [18].

It is worthy to mention that twinning influences the evolution of the deformed texture, because unlike the slip, it is a directional mechanism. Additionally, during the initial stages of the deformation process, it causes grain refinement. However, it retards further grain refinement during the next stages [19, 20].

3.2. Microhardness and recrystallization behavior

The microhardness values of the as-received CP Ti and cold-rolled samples at different rolling reduction percent are shown in Fig. 6. Increasing the rolling reduction and induced strain causes an increase in the hardness values of the samples. The hardness of the 90% cold-rolled samples is about 80% higher than that of the as-received sample. The hardening of the processed samples may be attributed to an increase in the dislocation

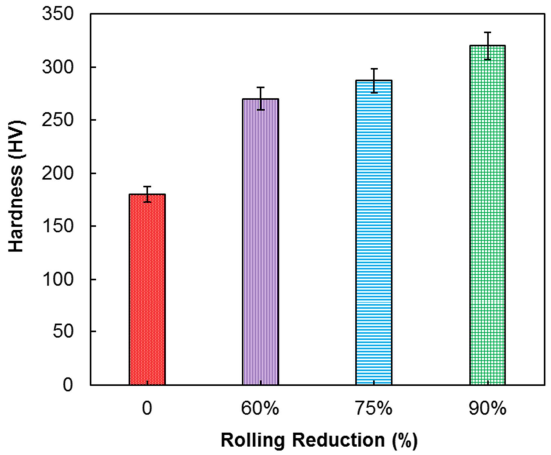

Fig. 6. Average microhardness of the as-received CP Ti and cold-rolled samples at different rolling reduction percent.

density, twinning phenomena, a significant reduction in grain size, and work-hardening. By increasing the rolling reduction, the amount of the LAGBs increases, which results in dislocation accumulation and consequently work-hardening phenomena [4, 13].

It should be noted that the increasing trend of the hardness is not constant for all of the reduction percentages. After 60% of the reduction occurs, the slope of the hardness variation is reduced. The as-received sample did not experience any type of mechanical treatment, so it had coarse grains. Thus, in the early stage of the cold-rolling process, the difference in grain size of the as-received and processed samples is significant. For a similar reason, the reduction rate of the grain size is too large in the early stages of cold-rolling. However, by increasing the reduction percentage of cold-rolling, due to the fact that the grains are already finer than the primary grains, the potential for decreasing the grain size weakens. The reason behind this is the gradual saturation of dislocations by the performance of more passes of the cold-rolling process. Macro- and micro-textures investigations on CP Ti indicated that increasing the rolling reduction up to 50% increases the intensity of the basal texture and further reduction decreases it [11, 21].

Pachla et al. [22] reported that the high strain-hardening rate of the titanium samples in the early stages of deformation could be related to the simultaneous occurrence of slipping and twinning. Ghosh et al. [23] concluded that the reason for improving the hardness of the rolled pure titanium is the direction of the applied force and the amount of change induced in the texture and structure of the sample. This change itself is related to the amount of occurrence of slipping and twinning formation in the sample.

Fig. 7 shows the results of microhardness measurements for the cold-rolled sample annealed at 500°C, and 700°C at different times. The microhardness trends show that for all of the annealing temperatures, the hardness decreases by lengthening the annealing process. Specifically, after 300 s of the annealing process, the hardness sharply reduced. It should be mentioned that annealing at 700°C had a larger impact

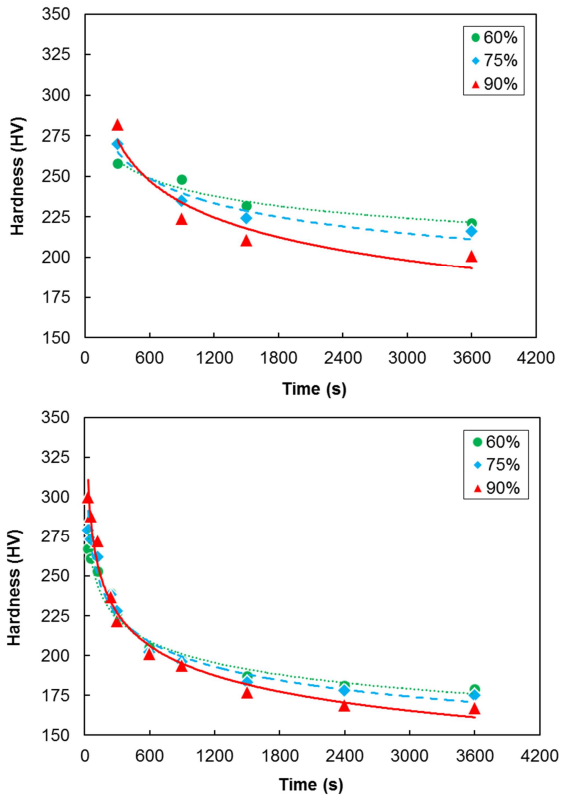

Fig. 7. The microhardness values and trends of the cold-rolled samples annealed at (a) 500°C, and (b) 700°C for different times.

on the softening of the cold-rolled sample. The hardness of the 90% cold-rolled sample decreased by almost 50% after 1 h annealing at 700°C. While, annealing at the same time and at 500°C, causes a drop of about 40% in the microhardness of the 90% cold-rolled sample. Increasing the temperature of the annealing process reduces the potential energy needed to overcome the activation energy of the nucleation to increase the recrystallization rate of the deformed α-phase. This causes the hardness to decrease by increasing the annealing temperature.

Moreover, at longer annealing times, the hardness drop is not significant, and the hardness changes approximately stood constant, which is in accordance with other studies [12]. At such times, a specific fraction of the deformed α-phase is already evolved completely, and all the deformed grains are fully recrystallized. Annealing at longer times only causes grain growth of the α-phase and consequently more hardness drop. A higher reduction percentage of the cold-rolling process

caused samples to rapidly soften, and to enter the grain growth zone in shorter times of the annealing process. This behavior can be explained as the consumed strain energy during the cold-rolling process. Since the strain energy is saved in the material in the forms of dislocations and other imperfections such as vacancies, higher deformation tends to increase the number of nucleation sites in the microstructure. This leads to an increase in the rate of the recrystallization phenomena [17].

Recrystallization is a result of nucleation and growth phenomena. The nucleation phenomena involve the nucleation of new grains, which induces no strain in the microstructure of the deformed sample. Since the density of dislocations is higher in the grain boundaries, the nucleation happens non-homogeneously. One of the accepted mechanisms for nucleation during recrystallization phenomena is the grain boundary migration caused due to the induced strain [4]. The volume fraction of the recrystallized α-grains (X_{rex}) is calculated using Eq. (2) [4]:

$$X_{rex} = \frac{H_0 - H_t}{H_0 - H_f} \qquad (2)$$

where H_0 is the microhardness of the deformed material, H_t is the microhardness of the annealed sample, and H_f is the hardness of the fully recrystallized sample. Considering Eq. (2), the volume fraction of the recrystallized phase is a function of the annealing time. The variations of the X_{rex} for the 90% cold-rolled sample annealed at three temperatures and different annealing times are plotted in Fig. 8. As it can be seen from Fig. 8, increasing the annealing time leads to an increase in the X_{rex}. Additionally, the X_{rex} was greater at higher annealing temperatures. It should be noted that at lower temperatures, an increase in annealing temperature has more effect on the recrystallized volume fraction. The strain rate, reduction percent, annealing temperature, concentration of the alloying elements, annealing time, and other thermal parameters are the important factors that affect the thermo-mechanical behavior of the metals [4].

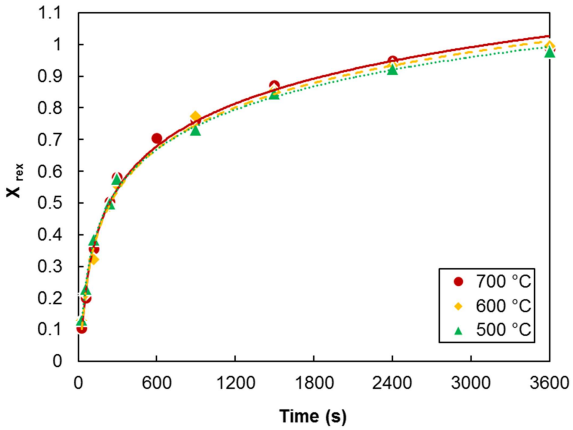

Fig. 8. The variation of the recrystallized volume fraction of the 90% cold-rolled sample at different temperatures and times.

Deformation of the material at room temperature causes the occurrence of static recrystallization (SREX) during annealing at high temperatures, in which new grains nucleate and grow. On the other hand, deformation of the material at high temperatures leads to dynamic recrystallization (DREX). The amount of strain induced to the material before the DREX, affects the kinetics of the SREX process. The amount of the induced strain also determines the density of dislocation. The dislocation density is considered as a necessary force that helps the recrystallization phenomena [4].

The process of the recrystallization phenomenon begins with a nucleation period. At this time, the nucleation of the new grains happens, and after that, by increasing the recrystallization rate, the nuclei begin to grow. As a result of colliding the grains, a decrease in dislocation density and reducing the growth rate causes the driving force to continue the recrystallization phenomena to decrease.

The Johnson-Mehl-Avrami-Kolomogrov (JMAK) model is a conventional model for investigating the kinetics of the recrystallization which is defined by Eq. (3) [4]:

$$X_{rex} = 1 - \exp(-kt^n) \qquad (3)$$

where t is the annealing time, k is the constant which depends on nucleation and growth processes, and n is the Avrami's exponent. The value of the n can be determined using the slope of Avrami's graph. Fig. 9

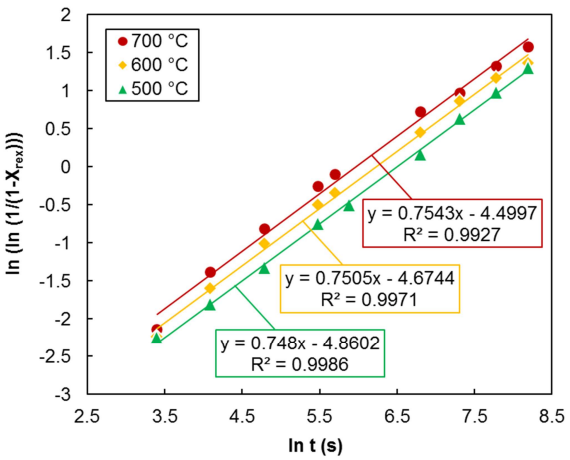

Fig. 9. Avrami's graphs for the 90% cold-rolled sample annealed at different temperatures and times.

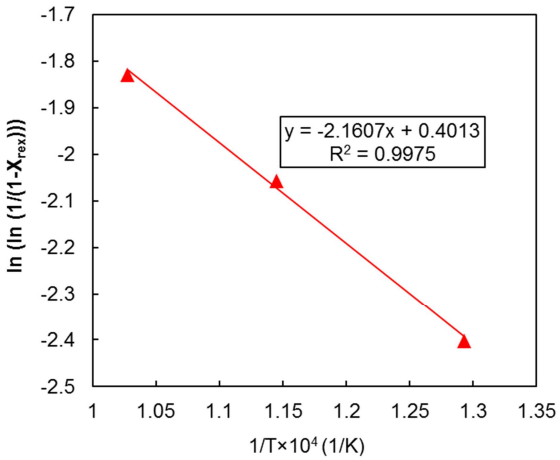

Fig. 10. The $\ln(\ln(1/(1-X_{rex}))$ versus $1/T$ curve for the 90% cold-rolled sample.

shows Avrami's graphs for the 90% cold-rolled sample annealed at different temperatures and times. In the case of the processes which are under the control of the diffusion the value of the n is in the range of 0.5-2.5 [24].

As mentioned before, the k constant depends on nucleation and growth processes which means it strongly depends on temperature. The relation between rate constant (k) and temperature (T) is defined as [25]:

$$k = A\exp\left(\frac{-Q}{RT}\right) \quad (4)$$

where Q is the activation energy, R is universal gaseous constant (8.314 J/mol.K), and A is a constant. By mixing the logarithmic forms of the Eqs. (3) and (4), the Eq. (5) can be derived:

$$\ln\left(\ln\left(\frac{1}{1-X_{rex}}\right)\right) = \ln A + n\ln t - \frac{Q}{RT} \quad (5)$$

In a constant annealing time, $\ln A + n\ln t$ can be considered constant. In this case, plotting the $\ln(\ln(1/1-X_{rex}))$ versus $1/T$ curve, results in a linear curve. The slope of this curve is equal to $-Q/R$. Fig. 10 shows this curve for the 90% cold-rolled sample. It should be noted that these mentioned theories are only acceptable for investigating the kinetics of recrystallization in the early stages.

Contieri et al. [12], by performing periodic optical microscopy on the microstructure of the highly cold-worked pure Ti, reported that the recrystallization activation energy of the mentioned sample is almost 165 kJ/mol. In the present study, this value was calculated to be about 179 kJ/mol for the 90% cold-rolled sample. The higher value for the activation energy calculated in this study can be attributed to the higher reduction percentage of the cold-rolling process. The values of Avrami's exponent and rate constant for the different reduction percentages and annealing temperatures calculated using the JMAK model are presented in Table 2. As can be seen, Avrami's exponent decreases by increasing the reduction percentage. But it is not a function of annealing temperature. In contrast, the rate constant increases by increasing both the reduction percentage and the annealing temperature.

Table 2. The values of the Avrami's exponent and rate constant for different thermo-mechanical conditions

Reduction percentage (%)	Annealing temperature (°C)	Avrami's exponent, *n*	Rate constant, *k*
60	700	0.9588	0.00141
75	700	0.9176	0.00169
90	500	0.7480	0.00775
90	600	0.7505	0.00933
90	700	0.7543	0.01111

3.3. Tensile properties

Fig. 11 shows the engineering stress-strain curves obtained by the tensile tests for as-received and cold-rolled samples. Moreover, the values of the mechanical properties of the samples are presented in Table 3. It can

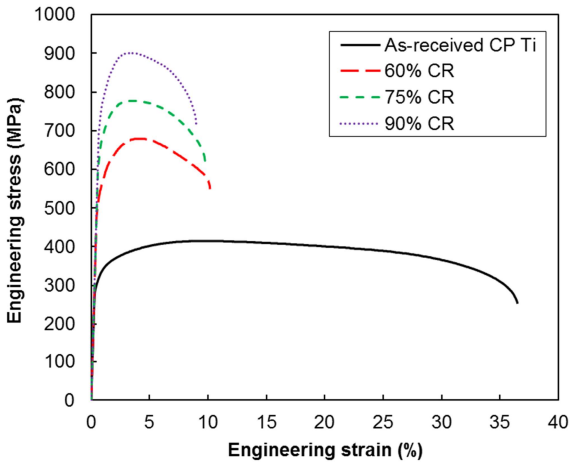

Fig. 11. The engineering stress-strain curves of the as-received and cold-rolled CP Ti samples after different reductions.

Table 3. Mechanical properties of the as-received and cold-rolled CP Ti samples

Sample	Yield Strength (MPa)	Ultimate Tensile Strength (MPa)	Elongation (%)
As-received CP Ti	280	415	36.4
60% cold-rolled	510	679	10.17
75% cold-rolled	620	777	9.75
90% cold-rolled	730	900	8.98

be observed that the strength of the samples increased significantly by performing the cold-rolling process. The yield strengths (YS) and ultimate tensile strengths (UTS) of the as-received Ti sample had an improvement of about 83% and 64%, respectively, by performing the 60% reduction via cold-rolling process. In addition, the elongation of the cold-rolled samples is much lower than that of the as-received sample. The elongation percentage of the 60% cold-rolled sample was almost 72% lower than that of the as-received sample. Increasing the reduction percentage of the cold-rolling process, gradually enhanced the YS and UTS. It also reduced the elongation of the samples. The YS and UTS of the 90% cold-rolled sample were 43% and 32% higher than those of the 60% cold-rolled sample. Inversely, the elongation percentage of the 90% cold-rolled sample was about 12% lower than that of the 60% rolled sample.

As shown in microhardness analysis, the significant enhancement in the YS and UTS of the samples can be attributed to the strain-hardening and grain refinement phenomena due to performing the cold-rolling process. The increase in dislocation density and more collides of the dislocations make the slip mechanism harder, which results in strain-hardening. Furthermore, the grain refinement phenomena occurred due to the formation of LAGBs and, subsequently, HAGBs, which leads to a decrease in the grain size of the samples [21, 26].

During the first stages of the cold-rolling process, the strain-hardening phenomena have a major effect on mechanical properties enhancement of the samples while the grain refinement phenomena have a minor role in this regard. On the other hand, during rolling at higher reduction percentages, the effect of strain hardening becomes less significant, and decreasing the grain size of the samples plays a more important role in improving the mechanical properties of the specimens. In addition, the decrease in ductility of the cold-rolled samples strongly results from the strain-hardening, which hinders the dislocation movement [27].

Figs. 12 and 13 present the stress-strain curves for the cold-rolled CP Ti samples at different reduction percentages (60%, 75%, and 90%) annealed at 500°C and 700°C, respectively. The curves were plotted for different annealing times of 5, 15, 25, and 60 min. Moreover, the values of the mechanical properties of the samples which were cold-rolled and annealed at mentioned conditions are given in Table 4. It can be seen from both figures that, in a constant reduction percentage, increasing the time of annealing, the UTS of the cold-rolled samples decreased. For instance, the UTS values of the 60% cold-rolled sample annealed at 500°C and 700°C decreased by about 16% by lengthening the annealing time from 5 min to 60 min. The changes in the UTS values of the 90% cold-rolled sample were approximately 21% in the same conditions of the annealing process. It should be noted that among the annealed samples, the 60% cold-rolled sample had the lowest UTS values in all of the annealing temperatures and times while the 90% cold-rolled sample had the highest UTS values in the same conditions.

However, the ductility of the samples was enhanced by performing the annealing process. For example, the elongation percentage of the 60% cold-rolled sample

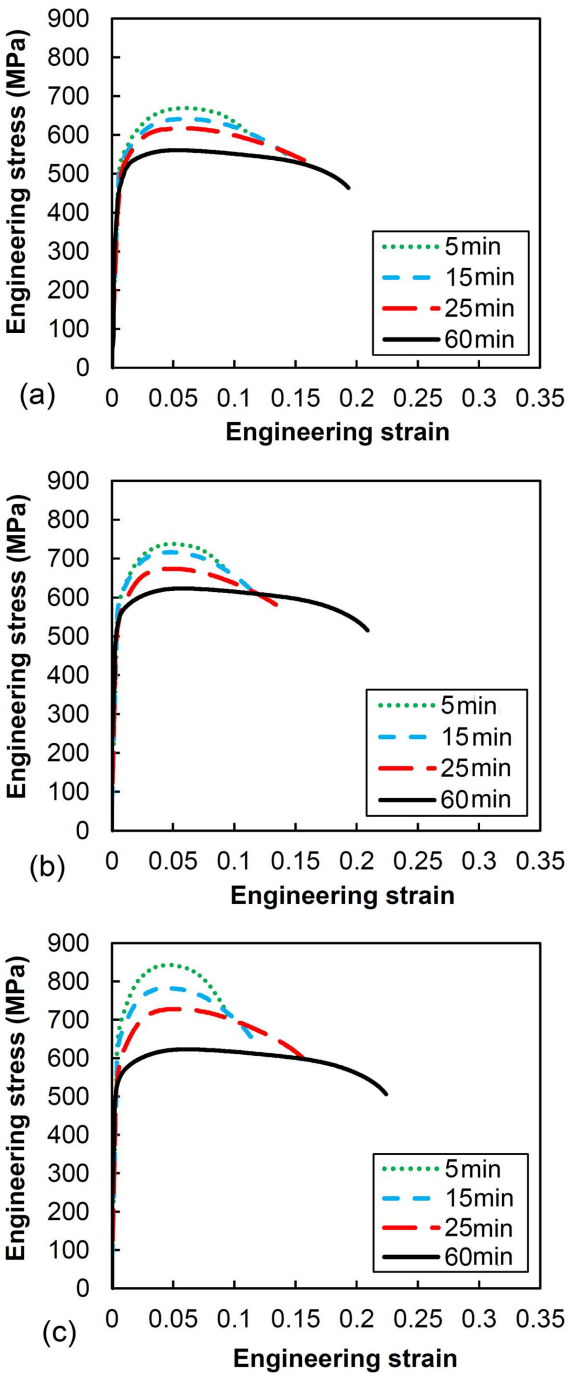

Fig. 12. The engineering stress-strain curves of the (a) 60%, (b) 75%, and (c) 90% cold-rolled samples annealed at 500°C for different times.

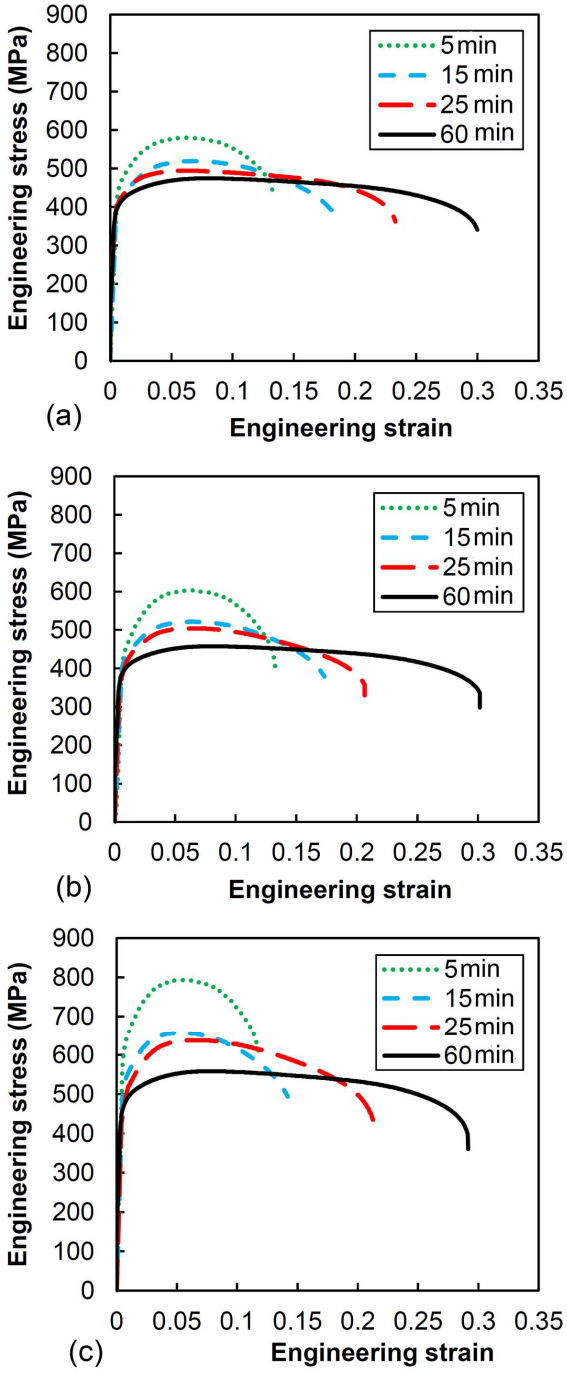

Fig. 13. The engineering stress-strain curves of the (a) 60%, (b) 75%, and (c) 90% cold-rolled sample annealed at 700°C for different times.

annealed at 500°C and 700°C, respectively. It increased at nearly 73% and 118% by lengthening the annealing time from 5 min to 60 min. In the case of the 90% cold-rolled sample, the changes were almost 137% and 138% at 500°C and 700°C, respectively. The minimum elongation percentage of the annealed samples at 500°C at different times belongs to the 90% cold-rolled sample. While, after annealing at 700°C for 1 h, the elongation percentages of the samples were nearly equal and higher than those of the samples annealed at 500°C. Due to the

Table 4. Mechanical properties of the cold-rolled samples annealed at different temperatures and times

Reduction percentage (%)	Property	Temperature (°C)	Time (s)			
			300	900	1500	3600
60	UTS (MPa)	500	669	642	616	560
75			737	716	673	623
90			843	783	738	662
60		700	565	530	515	474
75			550	525	510	457
90			715	656	637	558
60	Elongation (%)	500	11.17	14.2	16	19.3
75			9.47	11.47	13.58	20.89
90			9.46	11.69	15.92	22.4
60		700	13.73	18.88	23.34	30
75			13.74	17.32	20.64	29.45
90			12.22	14.2	21.3	29.15

fact that at 500°C the activation energy needed for recrystallization is higher than that of 700°C, the nucleation rate of the recrystallized grains is slower. Thus, the growth of these grains happens in longer times. Hence, it can be concluded that the minimum annealing time needed for developing new recrystallized grains with a desirable distribution at 500°C is 1 h.

Performing the annealing process at 700°C for 5 min resulted in the formation of a microstructure consisting of deformed and recrystallized α-grains. This microstructure leads to an increase in the UTS values of the cold-rolled samples. Despite the improvement in UTS values, annealing at longer times has led to an increase in the elongation of the cold-rolled samples. The annealing process at 700°C for 1 h led to the formation of a uniform distribution of α-grains in the microstructure of the cold-rolled CP Ti sheets. Formation of such microstructure results in significant improvement in the UTS and elongation of the cold-rolled samples. As can be inferred from the stress-strain curves, the thermo-mechanical process strongly affected the tensile strength and elongation of the specimens.

Terada et al. [28] studied the mechanical properties of the CP Ti sheets, which had been subjected to the accumulative roll bonding (ARB) process. They showed that applying six passes of the ARB process approximately causes a 7.3% decrease in the elongation of the samples. Performing the annealing process at 300°C on the ARB processed samples had no significant effect on their elongation. However, they showed annealing at 500°C caused about a 37% increase in the elongation percentage of the ARB processed samples because the recrystallization and recovery phenomena have been completely done, and the fine deformed α-grains are fully recrystallized during the annealing process.

The results of the tensile test performed in the present study proved that the proper mixture of the mechanical properties, including UTS and elongation, can be achieved by performing a suitable thermo-mechanical process on the CP Ti sheets.

3.4. Fracture behavior

The SEM micrographs from the fracture surfaces of the as-received CP Ti, 90% cold-rolled CP Ti before and after annealing are shown in Fig. 14. As can be seen from Fig. 14, the fracture surface of the samples consists of dimples. For each sample, the dimples are uniform in size and shape. The presence of dimples in the fracture surface of the samples indicates the ductile fracture of the titanium, which is typical for the fracture behavior of this metal at room temperature [21]. Generally, the ductile fracture of the metals during the tensile experiment occurs in three stages. Firstly, the microcavities nucleate under the tension forces. Secondly, they grow, and in the final stages, they merge to form so-called dimples [29].

Regarding Fig. 14(a), the fracture surface of the as-received CP Ti sample displays the large and shallow dimples which have a flat bottom. These characteristics

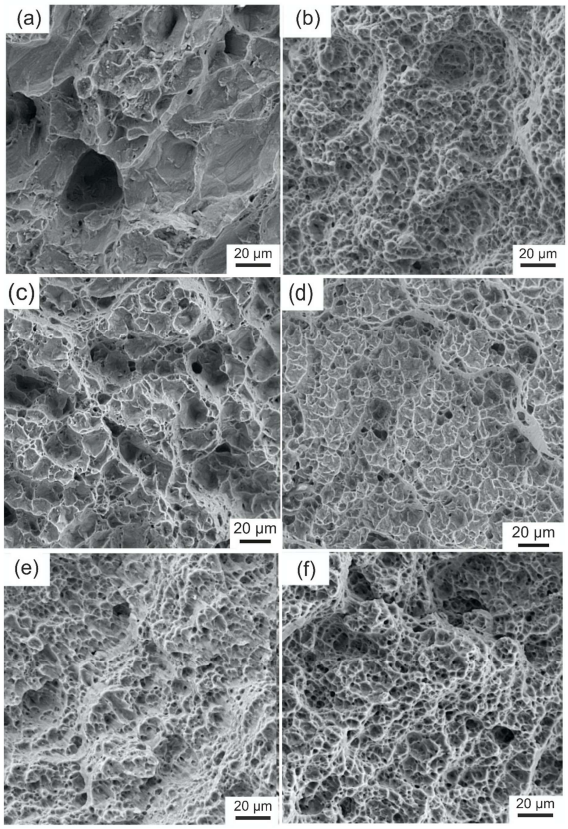

Fig. 14. SEM images from the fracture surface of the tensile samples: (a) as-received CP Ti, (b) 90% cold-rolled, (c) 90% cold-rolled and annealed at 500°C for 300 s, (d) 90% cold-rolled and annealed at 500°C for 3600 s, (e) 90% cold-rolled and annealed at 700°C for 300 s, and (f) 90% cold-rolled and annealed at 700°C for 3600 s.

of the dimples indicate for growing the cracks in the as-received sample, for which a low amount of energy is needed. The dimples lead to the formation of macroscopic and inter-granular cracks in the as-received sample.

The morphology of the 90% cold-rolled fracture surface is shown in Fig. 14(b). A large number of the shallow dimples and microcavities are visible in the fracture surface of the 90% cold-rolled sample. Due to the work-hardening in such a high reduction in thickness, the dislocation density and consequently the restored energy in grain boundaries of α-grains increase. The increase in restored energy of α-grain boundaries can be a suitable source for the nucleation of microcavities. Thus, the low ductility of the 90% cold-rolled sample can be attributed to the high number of microcavities. During the tensile test, these micro-cavities rapidly merge and cause the failure of the sample.

Figs. 14(c) to14(f) show SEM images from the fracture surface of the annealed samples. Fracture surfaces of the annealed samples at 500°C for 5 min and 1 h are shown in Figs. 14(c) and 14(d), respectively. In addition, SEM images taken from the fracture surfaces of the annealed samples at 700°C for annealing times of 5 min and 1 h are shown in Figs. 14(e) and 14(f), respectively.

After annealing at 500°C for 300 s, the fracture surface remains with relatively refined characteristics, while the size of the dimples increased and their number decreased (Fig. 14(c)). After annealing at 500°C for 3600 s, the nanoscale and ultrafine scale grains can effectively reduce the nucleation size of flaw and prevent crack propagation, resulting in the formation of fine and deeper dimples in the fracture surface, indicating ductile features (Fig. 14(d)) [30]. It seems annealing at 700°C, intensifies the mentioned characteristics and hence had a more effect on improving the ductility of the samples.

4. Conclusion

The mechanical and recrystallization behaviors of the pure titanium sheets deformed by the cold-rolling process in 60%, 75%, and 90% thickness reduction and annealed at different times and temperatures were investigated. Based on the results of this investigation, the following results can be obtained:

1. Optical microscopy indicated that after annealing, the number of twins significantly decreased and the recrystallized grains grew. Annealing at longer times causes more growth of recrystallized grains.
2. XRD analyses taken from the cold-rolled samples showed that by increasing the reduction percentages, the dislocation density in the samples increased while the crystallite size decreased.
3. Microhardness measurements indicated that the hardness of the rolled samples was enhanced up to 82% by increasing the reduction percentages of the cold-rolling process. Annealing makes the samples soft. Increasing the time and temperature of the

annealing had more effects on the softening of the samples. For instance, the 90% cold-rolled samples which experienced 1 h annealing at 500ºC and 700ºC had about 32% and 43% lower hardness than that of the as-received sheet, respectively.

4. The Johnson-Mehl-Avrami-Kolomogrov (JMAK) model was used to evaluate the recrystallization behavior of the samples. Avrami's exponent decreased from 0.96 to 0.75 by increasing the reduction percentage from 60% to 90%. But it did not vary with a change in the annealing temperature. In contrast, the rate constant increased by increasing both reduction percentage and annealing temperature.
5. Increasing the reduction percentage of the cold-rolling process, gradually enhanced the YS and UTS (up to 160% and 117%, respectively) while it reduced the elongation of the samples. For example, the elongation percentage of the 90% cold-rolled sample dropped by about 75%, regarding that of the as-received sheet. In a constant reduction percentage, by increasing the time and temperature of annealing the UTS of the cold-rolled samples decreased. However, the elongation of the cold-rolled samples was enhanced by performing the annealing process. The UTS and elongation percentage of the 90% cold-rolled sample annealed at 700ºC for 1 h reached to about 558 MPa and 29%, respectively. These values were about 415 MPa and 36% for the as-received sheet.

Acknowledgements

The authors gratefully acknowledge Bu-Ali Sina University for providing financial support during the research work.

Conflict of Interests

The authors declare that they have no known competing financial interests or personal relationships that could have appeared to influence the work reported in this paper.

5. References

[1] G. Lütjering, J. Williams, Titanium, Springer, Berlin, Heidelberg, 2003.

[2] I. Polmear, D. StJohn, J.F. Nie, M. Qian, Light alloys: metallurgy of the light metals, Butterworth-Heinemann, 2017.

[3] Y. Wang, W. He, N. Liu, A. Chapuis, B. Luan, Q. Liu, Effect of pre-annealing deformation on the recrystallized texture and grain boundary misorientation in commercial pure titanium, *Materials Characterization*, 136 (2018) 1-11.

[4] F.J. Humphreys, M. Hatherly, Recrystallization and related annealing phenomena, Elsevier, Pergamon Press, Oxford, 2012.

[5] G. Gottstein, Physical foundations of materials science, Springer-Verlag Berlin Heidelberg, 2004.

[6] S. Panda, S.K. Sahoo, A. Dash, M. Bagwan, G. Kumar, S.C. Mishra, S. Suwas, Orientation dependent mechanical properties of commercially pure (cp) titanium, *Materials Characterization*, 98 (2014) 93-101.

[7] S. Sinha, A. Ghosh, N.P. Gurao, Effect of initial orientation on the tensile properties of commercially pure titanium, *Philosophical Magazine*, 96(15) (2016) 1485-1508.

[8] D. Kuhlmann-Wilsdorf, Theory of plastic deformation:- properties of low energy dislocation structures. *Materials Science and Engineering: A*, 113 (1989) 1-41.

[9] B. Bay, N. Hansen, D.A. Hughes, D. Kuhlmann-Wilsdorf, Overview no. 96 evolution of fcc deformation structures in polyslip. *Acta Metallurgica et Materialia*, 40(2) (1992) 205-219.

[10] M.J. Phillippie, C. Esling, B. Hocheid, Role of twinning in texture development and in plastic deformation of hexagonal materials, *Texture, Stress, and Microstructure*, 7(4) (1988) 265-301.

[11] Y.B. Chun, S.H. Yu, S.L. Semiatin, S.K. Hwang, Effect of deformation twinning on microstructure and texture evolution during cold rolling of CP-titanium, *Materials Science and Engineering: A*, 398(1-2) (2005) 209-219.

[12] R.J. Contieri, M. Zanotello, R. Caram, Recrystallization and grain growth in highly cold worked CP-Titanium, *Materials Science and Engineering: A*, 527(16-17) (2010) 3994-4000.

[13] T. Ungár, J. Gubicza, G. Ribárik, A. Borbély, Crystallite size distribution and dislocation structure determined by diffraction profile analysis: principles and practical application to cubic and hexagonal crystals. *Journal of Applied Crystallography*, 34(3) (2001) 298-310.

[14] A. Fattah-alhosseini, M.K. Keshavarz, Y. Mazaheri, A.R. Ansari, M. Karimi, Strengthening mechanisms of nano-grained commercial pure titanium processed by accumulative roll bonding, *Materials Science and Engineering: A*, 693 (2017) 164-169.

[15] H.S. Kim, W.J. Kim, Annealing effects on the corrosion resistance of ultrafine-grained pure titanium, *Corrosion Science*, 89 (2014) 331-337.

[16] P. Sahu, M. De, S. Kajiwara, Microstructural characterization of stress-induced martensites evolved at low temperature in deformed powders of Fe-Mn-C alloys by the Rietveld method, *Journal of Alloys and Compounds*, 346(1-2) (2002) 158-169.

[17] R.E. Smallman, Modern physical metallurgy, Elsevier, 2016.

[18] A.O.F. Hayama, H.R.Z. Sandim, Annealing behavior of coarse-grained titanium deformed by cold rolling, *Materials Science and Engineering: A*, 418(1-2) (2006) 182-192.

[19] S. Nourbaksh, T.D. O'Brien, Texture formation and transition in cold rolled titanium, *Materials Science and Engineering*, 100 (1988) 109-114.

[20] S.V. Zherebtsov, G.S. Dyakonov, A.A. Salem, S.P. Malysheva, G.A. Salishchev, S.L. Semiatin, Evolution of grain and subgrain structure during cold rolling of commercial- purity titanium, *Materials Science and Engineering: A*, 528(9) (2011) 3474-3479.

[21] H. Nasiri-Abarbekoh, A. Ekrami, A.A. Ziaei-Moayyed, M. Shohani, Effects of rolling reduction on mechanical properties anisotropy of commercially pure titanium, *Materials & Design*, 34 (2012) 268-274.

[22] W. Pachla, M. Kulczyk, M. Sus-Ryszkowska, A. Mazur, K.J. Kurzydlowski, Nanocrystalline titanium produced by hydrostatic extrusion, *Journal of Materials Processing Technology*, 205(1-3) (2008) 173-182.

[23] A. Ghosh, A. Singh, N.P. Gurao, Effect of rolling mode and annealing temperature on microstructure and texture of commercially pure-titanium, *Materials Characterization*, 125 (2017) 83-93.

[24] J. Burke, The kinetics of phase transformations in metals, Pergamon Press INC, 1965.

[25] D.A. Porter, K.E. Easterling, Phase transformations in metals and alloys, Third Edition, CRC press, 2009.

[26] X. Li, Y.L. Duan, G. F. Xu, X. Y. Peng, C. Dai, L. G. Zhang, Z. Li, EBSD characterization of twinning in cold-rolled CP-Ti, *Materials Characterization*, 84 (2013) 41-47.

[27] L.I.U. Na, W.A.N.G. Ying, W.J. He, L.I. Jun, A. Chapuis, B.F. Luan, L.I.U. Qing, Microstructure and textural evolution during cold rolling and annealing of commercially pure titanium sheet, *Transactions of Nonferrous Metals Society of China*, 28(6) (2018) 1123-1131.

[28] D. Terada, S. Inoue, N. Tsuji, Microstructure and mechanical properties of commercial purity titanium severely deformed by ARB process, *Journal of Materials Science*, 42(5) (2007) 1673-1681.

[29] G.E. Dieter, D. Bacon, Mechanical metallurgy, New York: McGraw-hill, 1976.

[30] Y.M. Wang, E. Ma, M.W. Chen, Enhanced tensile ductility and toughness in nanostructured Cu, *Applied Physics Letters*, 80(13) (2002) 2395-2397.